

Optimization of Landmark Selection for Cortical Surface Registration

Anand Joshi

Signal and Image Processing Institute,
University of Southern California,
Los Angeles 90089, USA

ajoshi@sipi.usc.edu

Dimitrios Pantazis

Signal and Image Processing Institute,
University of Southern California,
Los Angeles 90089, USA

pantazis@sipi.usc.edu

Hanna Damasio

Dornsife Neuroscience Imaging Center
University of Southern California
Los Angeles, CA 90089, USA

hdamasio@college.usc.edu

David Shattuck

Laboratory of Neuro Imaging,
University of California, Los Angeles,
Los Angeles 90095, USA

shattuck@loni.ucla.edu

Quanzheng Li

Signal and Image Processing Institute,
University of Southern California,
Los Angeles 90089, USA

quanzhel@sipi.usc.edu

Richard Leahy

Signal and Image Processing Institute,
University of Southern California,
Los Angeles 90089, USA

leahy@sipi.usc.edu

Abstract

Manually labeled landmark sets are often required as inputs for landmark-based image registration. Identifying an optimal subset of landmarks from a training dataset may be useful in reducing the labor intensive task of manual labeling. In this paper, we present a new problem and a method to solve it: given a set of N landmarks, find the $k (< N)$ best landmarks such that aligning these k landmarks that produce the best overall alignment of all N landmarks. The resulting procedure allows us to select a reduced number of landmarks to be labeled as a part of the registration procedure. We apply this methodology to the problem of registering cerebral cortical surfaces extracted from MRI data. We use manually traced sulcal curves as landmarks in performing inter-subject registration of these surfaces. To minimize the error metric, we analyze the correlation structure of the sulcal errors in the landmark points by modeling them as a multivariate Gaussian process. Selection of the optimal subset of sulcal curves is performed by computing the error variance for the subset of unconstrained landmarks conditioned on the constrained set. We show that the registration error predicted by our method closely matches the actual registration error. The method determines optimal curve subsets of any given size with minimal registration error.

1. Introduction

Registration of images consists of computing a transformation between two acquisitions, or equivalently, determining the point-to-point correspondence between the images [1, 2]. Registration algorithms are usually based either on aligning features extracted from the image or on the optimization of a similarity measure of the image intensities [3]. Landmarks are typically points or curves that are either labeled manually or extracted automatically from the image data [2, 4, 5, 6, 7]. Manual demarcation of landmarks can be a labor-intensive task, and therefore the set of landmarks to be labeled should be optimized. The locations of landmarks in the images imposes a correlation in them which can be used to reduce the size of the landmark set. In this paper, we explore the problem: given a set of N candidate landmark points, what is the best subset of k landmarks, from $\binom{N}{k}$ possible choices of such subsets? We discuss this problem as applied to the problem of sulcal set optimization for registration of cerebral cortices of human brains.

The cerebral cortex, or simply the cortex of the brain plays a key role in memory, attention, perceptual awareness, thought and language. The human cerebral cortex is 2 – 4 mm thick and thus for many applications it can be modeled

as a surface rather than a volume. A sulcus is a depression or fissure in the cortex and is closely related to the function of the brain. Cortical surface registration has important applications in cross-sectional and longitudinal neuroanatomical studies, for example mapping and analyzing progression of disorders such as Alzheimer’s disease [8] and studying growth patterns in developing human brains [9, 10]. There are two main categories of methods that align the cortex from a subject to an atlas: manual landmark based methods [11] and automatic methods based on alignment of geometric features [12, 13] or surface indices [14]. The main advantage of automatic methods is that there is no manual input required for performing the alignment. However they may be less reliable in the sense that they do not incorporate higher level knowledge of sulcal anatomy. Certain sulcal and gyral patterns are hard to identify automatically based on local geometric features, therefore expert delineation of such landmarks can be useful for accurate registration. The objective of landmark based manual registration methods is to minimize the misalignment error in the sulcal curves. Moreover, they allow the users to mark additional structures in certain areas of interest in order to achieve more control for accurate alignment in those regions. A disadvantage of the manual approaches is that the individual tracers need to be trained, and even then inter-rater variability introduces some uncertainty into the procedure. Additionally, for large scale studies, manual procedures may be infeasible unless we minimize the number of sulcal curves required in the manual tracing protocol. It is this latter issue that we address here.

We begin with a large set of sulcal curves that have been identified by the neuroanatomist on our team as candidate landmarks for cortical registration. Our objective is to select an optimal subset from this set such that, for a given number of curves, the sulcal registration error is minimized when computed over all sulci. One straightforward approach is to actually perform registration of the sulcal curves for a set of training images using all possible subsets and then measure the error in the remaining unconstrained sulcal curves. The difficulty with this approach is that there are a huge number of combinations possible. In our case we have 27 candidate curves. Supposing we want to define a protocol that uses 10 curves, the number of combinations to be tested is $\binom{27}{10} \approx 8.4$ million. If the error is to be estimated by performing pairwise registrations of 20 brains, i.e. $\binom{20}{2}$ registrations, then the total number of registrations required is $\binom{20}{2} \binom{27}{10} \approx 1.6$ billion. This is a prohibitively large number.

Instead of performing actual brain registrations with multiple subsets of constrained sulci, we perform only pairwise unconstrained registrations using the elastic energy minimization procedure described in [11]. The resulting maps produce reasonable correspondences so that we can model the measured sulcal registration errors using a mul-

tivariate Gaussian distribution. Using conditional probabilities, we then analytically predict the registration error that would result if we constrained a subset of the curves to match using hand-labeled sulci. These errors can be rapidly computed using conditional covariances, and as we show below, lead to reasonably accurate estimates of the true errors that result when constraining the curves. For a fixed number of constrained curves, we estimate the errors for all possible subsets of that size and select the one with the smallest predicted error. We investigate the prediction accuracy of our model by doing actual registrations using the optimal sulcal constraint set. No searching strategy is required in our method, because for a particular subset of curves, our method gives an analytical expression for the registration error. This expression can be easily calculated for all possible subsets eliminating the need for a search.

2. Surface Registration Method

A class of surface registration based methods use an intermediate parameter space, either a square [8, 11] or a sphere [15], on which the sulcal landmarks or shape based features are aligned. In this paper, we use the flat-mapping surface registration method described in [11], however the same framework is readily adaptable to other surface registration methods [16, 17]. The details of the flat mapping based method are outlined in [11, 18].

Flat mapping based registration methods, combined with the highly variable cortical anatomy, introduce inherent correlation patterns in the locations of unconstrained sulci. In our maps to the unit square we map the corpus callosum to the edges of the unit square causing uneven deformations in different cortical regions, with the temporal lobe mapping to a much smaller area than the medial cortex for instance. Furthermore, minimizing elastic energy deforms the cortical anatomy in a smooth fashion so that one would expect to see significant correlations between sulcal errors in neighboring sulci. Our method takes advantage of this correlation structure to create a multivariate Gaussian model of sulcal registration errors when no curves are constrained. We then predict these errors when some sulci are constrained using conditional probabilities.

2.1. Sulcal Curves, Flat Mapping and Alignment

We used the BrainSuite software [19] to interactively trace the $N = 27$ candidate sulci depicted in Fig. 1 on both hemispheres of each of the 12 brains used in this study. The surface based registration method we used here performs simultaneous parameterization and registration of the manually traced sulcal landmarks. In order to generate such a flat map with prealigned sulcal curves, we model the cortical surface as an elastic sheet and solve the associated linear elastic equilibrium equation using the finite element method (FEM). Let $\phi = [\phi_1, \phi_2]$ be the two coordinates assigned to

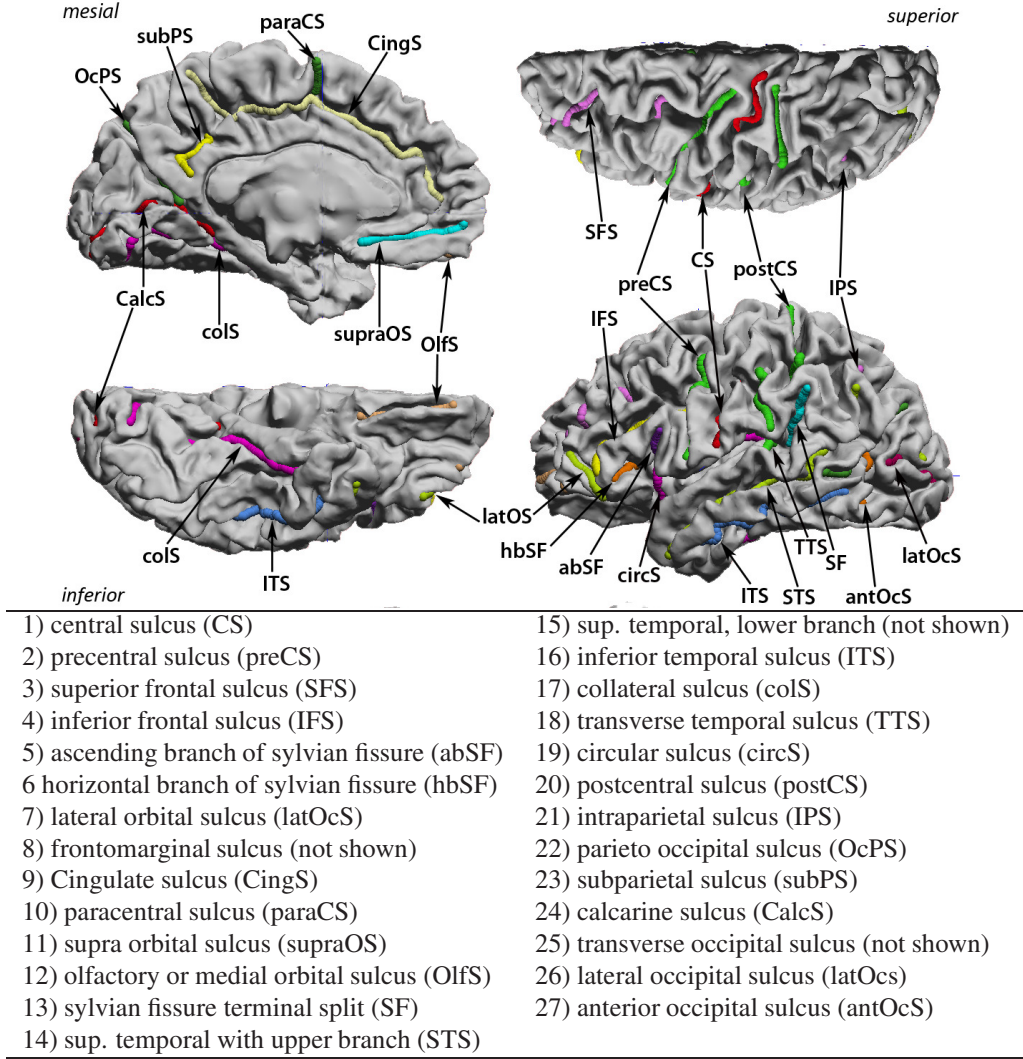


Figure 1. The complete set of candidate sulcal curves from which we select an optimal subset for constrained cortical registration

every point on a given cortical surface such that the coordinates ϕ satisfy the linear elastic equilibrium equation with Dirichlet boundary conditions on the boundary of each cortical hemisphere, represented by the corpus callosum. We constrain the corpus callosum to lie on the boundary of the unit square mapped as a uniform speed curve. The elastic strain energy $E(\phi)$ is given by:

$$E(\phi) = \int_S \frac{\mu}{2} \text{Tr}(((D\phi)^T + D\phi)^2) + \lambda \text{Tr}(D\phi)^2 dS, \quad (1)$$

where $D\phi$ is the covariant derivative of the coordinate vector field ϕ . Let ϕ_{B_1} and ϕ_{B_2} denote the 2D coordinates to be assigned to corresponding hemispheres of two brains denoted by B_1 and B_2 respectively. We then define the Lagrangian cost function $C(\phi_{B_1}, \phi_{B_2})$ as

$$C(\phi_{B_1}, \phi_{B_2}) = E(\phi_{B_1}) + E(\phi_{B_2}) + \sigma^2 \sum_{k \in C} (\phi_{B_1}(x_k) - \phi_{B_2}(y_k))^2, \quad (2)$$

where $\phi_{B_1}(x_k)$ and $\phi_{B_2}(y_k)$ denote the coordinates assigned to the sulcal landmarks $x_k \in B_1$, $y_k \in B_2$ and σ^2 is a Lagrange multiplier. The landmarks correspond to uniformly sampled points along each sulcal curve. We refer the reader to [11, 18] for implementation details. We use $\sigma^2 = 0$ for unconstrained registration, which is used for estimation of the covariance of the sulcal registration errors, as described later. We then analytically predict the errors when some sulci are constrained, without doing actual constrained registrations, using conditional densities as described below. To test the accuracy of our predictions, we perform registrations with $\sigma^2 = 10$ and C the set of constrained sulci, a subset of the 27 available curves. This method results in a bijective map of each brain hemisphere to unit squares such that the constrained sulci match in the flat space (Fig. 2a). The point correspondence from one

cortical surface hemisphere to the other is then obtained using the coordinate system of the common mapping to the unit square.

2.2. Registration Error

For every pair of registered hemispheres, we map the traced curves of one brain to the other, which is arbitrarily defined as a target. The registration used is either unconstrained for error prediction, or constrained for validation. We parameterize each sulcal curve n over $s \in [0, 1]$ and then compute the point-to-point average error $\mathbf{e}_n = \text{mean}_s\{\mathbf{e}_n(s)\}$, as illustrated in Fig. 2, where $\mathbf{e}_n(s)$ is the registration error in 3D coordinates for location s on the n^{th} curve. For symmetry, we repeat the procedure by interchanging subject and target brains.

The alignment error in a sulcus causes a registration error in the surrounding cortical area. Therefore, isolated sulci will have more impact on registration, since their misregistration will affect large cortical regions. To compensate for this effect, we parcellate the cortex into $N = 27$ regions by assigning each cortical point to the nearest sulcal curve (Fig 2b). The parcellation was performed for all $M = 24$ available brain hemispheres. We then defined a weight function for the n^{th} sulcus to be $w_n = \frac{1}{M} \sum_{i=1}^M A_n^i / A^i$, where A_n^i is the surface area of the n^{th} parcellated region in the i^{th} brain, and A^i is the total surface area of the i^{th} hemisphere.

Finally, the surface registration error metric was defined as

$$E_R = \mathbb{E} \left(\sum_n w_n (e_n^x)^2 + w_n (e_n^y)^2 + w_n (e_n^z)^2 \right), \quad (3)$$

where e_n^x, e_n^y and e_n^z represents the x, y , and z components of \mathbf{e}_n , and $\mathbb{E}(\dots)$ is the expectation operator. Alternatively, the errors could be calculated with respect to surface geometry rather than in 3D. While calculating errors based on geodesic distances is an interesting possibility, they are very difficult to model statistically because geodesics do not form a vector space. When the geodesic errors are small, they could be approximated by errors in 3D, as is done in this paper. Below, we substitute $E_n^x = \sqrt{w_n} e_n^x$ in order to simplify subsequent analysis. The objective of the surface registration procedure is to minimize this registration error E_R .

3. Probabilistic Model of the Sulcal Errors

We model the sulcal errors E_1^x, \dots, E_N^x as jointly Gaussian random variables, since these errors are drawn from a large population of brain pairs. We describe computations for the x component of the error; similar computations are performed for y and z . The distribution model of E_j^x for

$j \in \{1, \dots, N\}$ is:

$$f_{E^x}(E_1^x, \dots, E_N^x) = \frac{1}{(2\pi)^{N/2} |\Sigma^x|^{1/2}} \exp \left(-\frac{1}{2} E^{xT} (\Sigma^x)^{-1} E^x \right) \quad (4)$$

where Σ^x denotes the covariance matrix of E^x . Therefore, the registration error can be expressed as:

$$E_R^x = \mathbb{E} \left\{ \sum_{i=1}^N (E_i^x)^2 \right\} = \text{Tr} (\Sigma^x) \quad (5)$$

We now want to predict the registration error when some of the sulci are explicitly constrained to register. We partition the curves into two sets: sulci F which are free and sulci N which are constrained so that $\{1 \dots N\} = F \cup C$. We assume that the registration algorithm is well behaved in a sense that it does not create unnatural deformations on the unconstrained sulci when a subset of them are constrained. In other words, if we constrain some sulci to register, the distribution of the remaining ones would be the same as if the constrained ones matched simply by chance, conditioned on the constrained sulci having zero error. Therefore, we model the registration errors in unconstrained sulci as the conditional distribution of the original joint Gaussian density. The probability density of a jointly Gaussian vector, conditioned on some of its elements being zero, is also jointly Gaussian. Therefore, the registration error E_R^{xc} after matching the sulci from C can be obtained using the conditional expectation:

$$E_R^{xc} = \mathbb{E} \left(\sum_{i \in F} E_i^{x2} | E_j^x = 0 \forall j \in C \right) = \text{Tr} (\Sigma_C^x) \quad (6)$$

where Σ_C^x is the conditional covariance matrix of the error terms corresponding to free sulci. By rearranging sulci so that free sulci precede the constrained ones, we can partition the covariance matrix as:

$$\Sigma^x = \begin{pmatrix} \Sigma_{ff}^x & \Sigma_{fc}^x \\ \Sigma_{cf}^x & \Sigma_{cc}^x \end{pmatrix}. \quad (7)$$

where Σ_{ff}^x and Σ_{cc}^x are the error covariances for free sulci and constrained sulci respectively, and Σ_{fc}^x and Σ_{cf}^x are the cross-covariances.

The conditional covariance is given by:

$$\Sigma_C^x = \Sigma_{ff}^x - \Sigma_{fc}^x (\Sigma_{cc}^x)^{-1} \Sigma_{cf}^x. \quad (8)$$

which is the Schur complement of Σ_{cc}^x in Σ^x [20]. The estimated registration error E_R^{xc} after constraining a subset of sulci is then:

$$E_R^{xc} = \text{Tr} (\Sigma_C^x). \quad (9)$$

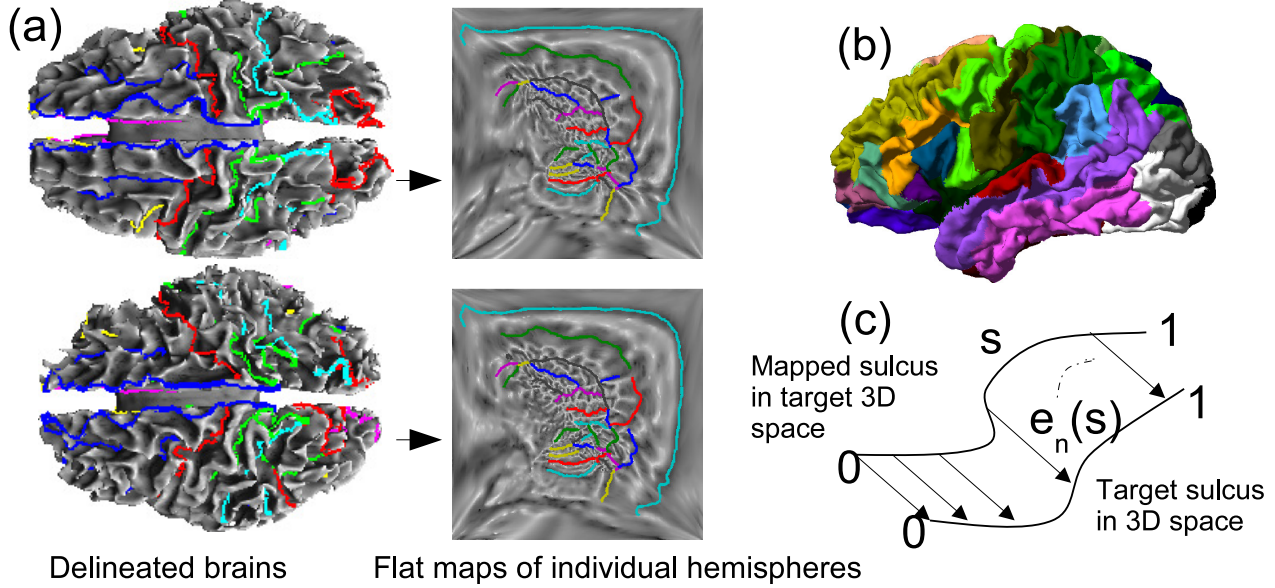


Figure 2. (a) Registration of two cortical surfaces based on the flat mapping method; (b) Parcellation of the cortex into regions surrounding the traced sulci; (c) Registration error for two corresponding sulci.

This formula allows us to estimate the x component of the registration error for a particular combination of constrained sulci and free sulci. The total registration error is evaluated by adding the x,y, and z components.

$$E_R^c = \text{Tr}(\Sigma_C^x) + \text{Tr}(\Sigma_C^y) + \text{Tr}(\Sigma_C^z). \quad (10)$$

We use this formula to estimate the total registration errors for all $\binom{N}{N_c}$ combinations of sulcal subsets, where N_c is the number of constrained sulci, and choose the subset that minimizes this error.

4. Results

A total of 12 brains, or equivalently 24 hemispheres, were delineated by trained raters. Our tracings, consisting of 27 candidate sulci per hemisphere (Fig. 1), were verified and corrected whenever necessary by one of the authors, an expert neuroanatomist. We performed unconstrained mappings for all 24 hemispheres by directly minimizing Eq. 1 for each hemisphere separately, instead of doing pairwise registrations using Eq. 2 with $\sigma = 0$, since the optimization in 2 becomes separable in the unconstrained case $\sigma = 0$. Using the flat maps of the 24 hemispheres we computed pairwise registration errors E_n^x , E_n^y , and E_n^z for all possible combinations of left and right hemispheres as described in Sec. 2.2. The resulting sample covariances are shown in Fig. 3.

By applying Eq. 10 to all subsets of a given number of constrained curves, we identified the subset that minimizes the registration error. The optimal subsets of curves

are given in Fig. 3 for numbers of constrained sulci from 1 to 27. We also calculated the sulcal registration errors for each of these optimal subsets by doing actual registrations. Comparing estimated and actual registration errors, also in Fig. 3, we see that the predicted values are close to those obtained when actually constraining the curves.

We performed a Lilliefors test which rejected the null hypothesis of normality for the errors E_n^x , E_n^y , and E_n^z for many sulci. This was not surprising because the finite size of brains, and therefore the registration error, is bounded. Consequently, a small deviation from normality was expected. However, the distributions were unimodal and the predicted errors of our model are in accordance with the actual ones, which indicates that our assumptions are in the sense of achieving the desired minimum error behavior.

To further test our method, we manually selected the set of 6 sulci with indices (3,12,24,1,9,21) to be constrained, which seemed a reasonable a priori selection based on sulcal extent and spatial distribution around the cortex. The algorithm predicted an error of $67.72mm^2$ and the actual error was $64.19mm^2$. The optimal set (3,14,16,17,21,24) found by our method had predicted an error of $36.77mm^2$ and the actual error was $34.46mm^2$, which is significantly better than our manually selected subset. We anticipate that in general the curves selected by our method should be superior to those selected on an intuitive basis, since various confounding effects due to elastic flat mapping as well as correlations in errors are accounted for in the algorithm.

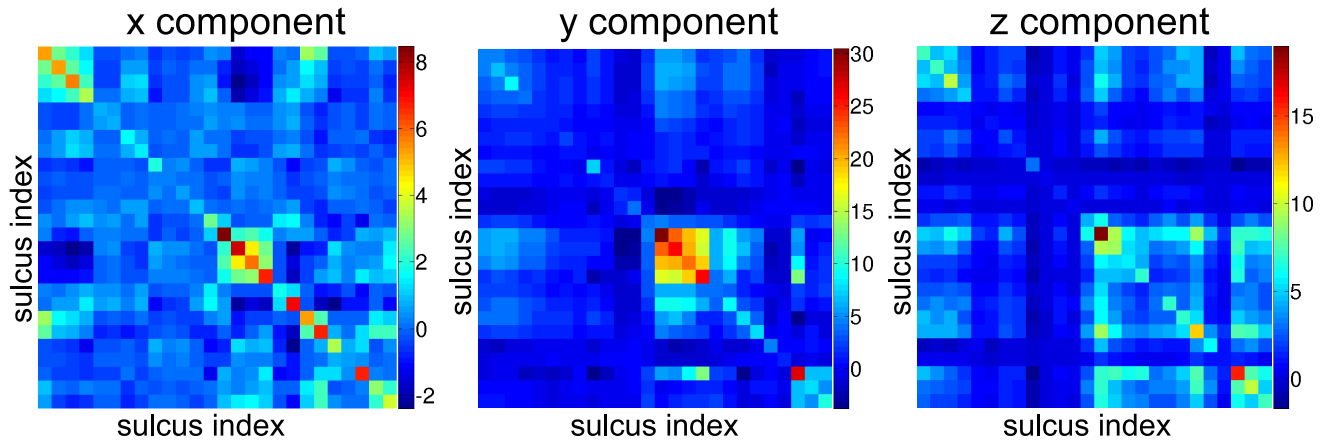


Figure 3. Sample covariance matrices for the x, y, and z components of the error represented as color coded images.

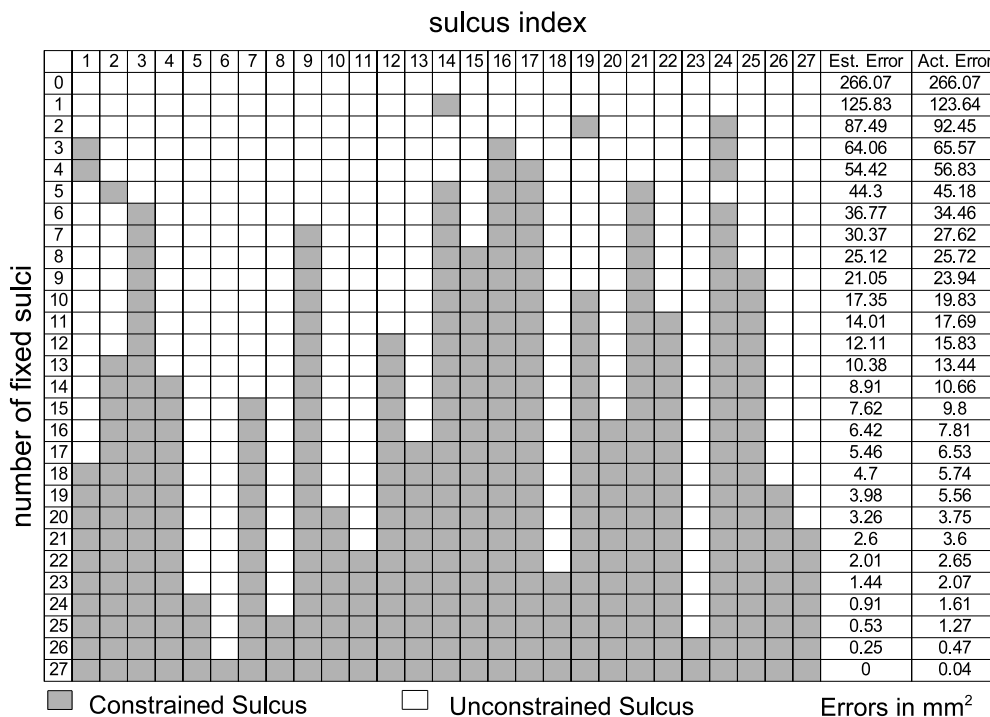


Figure 4. Each row gives the indices of the optimal subset of sulci that minimize the registration error against all other combinations with equal number of constrained curves. The two right columns show that the estimated (est.) error is close to the calculated (act.) error when actual registrations with the same constrained curves are performed.

5. Discussion

We have described a general procedure for selecting subsets of sulcal landmarks for use in constrained cortical registration. The procedure can be used to reduce the time required for manual labeling of sulci in group studies of cortical anatomy and function.

Notice that the central sulcus is not selected for proto-

cols with a small number of curves (less than 6). This is probably because the sulci that are most stable and consistent among brains, such as the central sulcus, may tend to align well even without explicitly aligning them. Therefore they may not improve the registration error significantly to justify their inclusion in the tracing protocol. Furthermore, short sulci neighboring other candidate curves are not pre-

ferred by the algorithm. For example, the paracentral sulcus, which is close to the cingulate sulcus, and the subparietal sulcus, which is close to the cingulate and the parieto-occipital sulcus are not preferred by the method. The algorithm tends to prefer long and variable sulci which are spatially distributed over different regions of the brain. This is consistent with intuition since the curves selected this way will help in overall brain registration.

Finally, we note that the methodology presented here readily extends to other landmark based registration methods in which the goal is to select an optimal subset of given size. This can greatly reduce the manual landmark labeling time for large scale studies. It can possibly be applied to other areas of computer vision [21, 22, 23, 24] for aiding optimal landmark selection.

References

- [1] Zitova, B., Flusser, J.: Image registration methods: a survey. *Image and Vision Computing* **21**(11) (October 2003) 977–1000
- [2] Brown, L.G.: A survey of image registration techniques. *ACM Computing Surveys* **24**(4) (1992) 325–376
- [3] Maintz, A.J.B., Viergever, M.A.: A survey of medical image registration. *Medical Image Analysis* **2**(1) (March 1998) 1–36
- [4] Rohr, K., Sprengel, R., Stiehl, H., et al.: Incorporation of landmark error ellipsoids for image registration based on approximating thin-plate splines. In: *Proc. Computer Assisted Radiology and Surgery (CAR'97)*, Berlin, Germany, June. (1997) 25–28
- [5] Chui, H., Rambo, J., Duncan, J., Schultz, R., Rangarajan, A.: Registration of cortical anatomical structures via robust 3D point matching. *Lecture Notes in Computer Science* (1999) 168–181
- [6] Besl, P., McKay, H.: A method for registration of 3-D shapes. *IEEE Transactions on pattern analysis and machine intelligence* **14**(2) (1992) 239–256
- [7] Chui, H., Rangarajan, A.: A new point matching algorithm for non-rigid registration. *Computer Vision and Image Understanding* **89**(2-3) (2003) 114–141
- [8] Thompson, P.M., Mega, M.S., Vidal, C., Rapoport, J., Toga, A.W.: Detecting disease-specific patterns of brain structure using cortical pattern matching and a population-based probabilistic brain atlas. In: *IPMI2001. LNCS* (2001) 488–501
- [9] N. Gogtay et al.: Dynamic mapping of human cortical development during childhood through early adulthood. *PNAS* **101** (2004) 8174–8179
- [10] Jeffery, K.J.: Learning of landmark stability and instability by hippocampal place cells. *Neuropharmacology* **37**(4-5) (1998) 677–687
- [11] Joshi, A.A., Shattuck, D.W., Thompson, P.M., Leahy, R.M.: Surface-constrained volumetric brain registration using harmonic mappings. *IEEE Trans. Med. Imaging* **26**(12) (2007) 1657–1669
- [12] Wang, Y., Chiang, M.C., Thompson, P.M.: Automated surface matching using mutual information applied to Riemann surface structures. In: *MICCAI 2005, LNCS* 3750. (2005) 666–674
- [13] Fischl, B., Sereno, M.I., Tootell, R.B.H., Dale, A.M.: High-resolution inter-subject averaging and a coordinate system for the cortical surface. *Human Brain Mapping* **8** (1998) 272–284
- [14] Tosun, D., Rettmann, M.E., Prince, J.L.: Mapping techniques for aligning sulci across multiple brains. *Medical Image Analysis* **8**(3) (2005) 295–309
- [15] Hurdal, M.K., Stephenson, K., Bowers, P.L., Summers, D.W.L., Rottenberg, A.: Coordinate system for conformal cerebellar flat maps. *NeuroImage* **11** (2000) S467
- [16] Thompson, P.M., Mega, M.S., Toga, A.W.: Disease-specific probabilistic brain atlases. In: *Proceedings of IEEE International Conference on Computer Vision and Pattern Recognition*. (2000) 227–234
- [17] Ju, L., Hurdal, M.K., Stern, J., Rehm, K., Schaper, K., Rottenberg, D.: Quantitative evaluation of three cortical surface flattening methods. *NeuroImage* **28**(4) (2005) 869–880
- [18] Joshi, A.A., Shattuck, D.W., Thompson, P.M., Leahy, R.M.: A finite element method for elastic parameterization and alignment of cortical surfaces using sulcal constraints. In: *Proc. of ISBI*. (2007)
- [19] Shattuck, D.W., Leahy, R.M.: Brainsuite: An automated cortical surface identification tool. *Medical Image Analysis* **8**(2) (2002) 129–142
- [20] Mardia, K., Kent, J., Bibby, J.: *Multivariate Analysis*. Academic Press (1979)
- [21] Madsen, C.B., Andersen, C.S. *Journal of Robotics and Autonomous Systems* **23** (1998) 277–292

- [22] Olson, C.: Landmark selection for terrain matching. In Proceedings of the IEEE International Conference on Robotics and Automation (2000) 1447–1452
- [23] Greiner, R., Isukapalli, R.: Learning to select useful landmarks. In: National Conference on Artificial Intelligence. (1994) 1251–1256
- [24] End, G., Treuer, H., Boesecke, R.: Optimization and evaluation of landmark-based image correlation. *Phys. Med. Biol.* **37** (1992) 261–271